



# CHORUS

This is the accepted manuscript made available via CHORUS. The article has been published as:

## Phonons in Si<sub>24</sub> at simultaneously elevated temperature and pressure

Xiao Tong, Xiaolin Xu, B. Fultz, Haidong Zhang, Timothy A. Strobel, and Duck Young Kim

Phys. Rev. B **95**, 094306 — Published 20 March 2017

DOI: [10.1103/PhysRevB.95.094306](https://doi.org/10.1103/PhysRevB.95.094306)

# Phonons in Si<sub>24</sub> at simultaneously elevated temperature and pressure

Xiao Tong,<sup>\*</sup> Xiaolin Xu,<sup>†</sup> and B. Fultz<sup>‡</sup>

*Department of Applied Physics and Materials Science,  
California Institute of Technology, Pasadena, CA 91125, USA*

Haidong Zhang<sup>§</sup> and Timothy A. Strobel<sup>¶</sup>

*Geophysical Laboratory, Carnegie Institution of Washington, Washington, DC 20015, USA*

Duck Young Kim<sup>\*\*</sup>

*Geophysical Laboratory, Carnegie Institution of Washington, Washington, DC 20015, USA and  
Center for High Pressure Science and Technology Advanced Research (HPSTAR), Shanghai 201203, China*

Raman spectroscopy was used to measure the frequencies of phonons in Si<sub>24</sub> with an open clathrate structure at temperatures from 80 K to 400 K, with simultaneous pressures of 0 to 8 GPa. The frequency shifts of the different phonons were substantially different under either temperature or pressure. The quasiharmonic behavior was isolated by varying pressure at low temperature, and the anharmonic behavior was isolated by varying temperature at low pressure. Phonon modes dominated by bond bending were anomalous, showing stiffening with temperature and softening with pressure. Both the quasiharmonic behavior and the anharmonic behavior changed markedly with simultaneous changes in temperature,  $\Delta T$ , and pressure,  $\Delta P$ . With  $\Delta T=320$  K and  $\Delta P=8$  GPa, some frequency shifts that scaled with the product  $\Delta T \Delta P$  were as large as the shifts from  $\Delta T$  and  $\Delta P$  alone. The thermodynamic entropy of this material likely has a dependence on  $\Delta T$  and  $\Delta P$  that cannot be obtained by adding effects from quasiharmonicity and phonon-phonon anharmonicity.

## I. INTRODUCTION

### I.1. Silicon

For any material there exists a causal relationship between structure and properties, whereby different modifications of the same composition may exhibit strikingly different attributes. For the case of silicon, the thermodynamic ground state at ambient conditions is the diamond cubic (DC) phase. This structure possesses an indirect band gap of 1.1 eV, and combined with a stable native oxide layer and large elemental abundance, DC-Si is arguably the most important semiconducting material in modern technology. Long-standing questions for silicon remain relevant, however, particularly with regard to overcoming intrinsic limitations of the fundamental indirect band gap. The integration of optical and electronic function on a single silicon wafer has been of enduring interest to the semiconductor industry<sup>1-4</sup>, for example, and many recent calculations suggest metastable, low-energy forms of silicon with properties that could potentially accommodate this possibility (see for example<sup>5-9</sup>).

Recently, a new allotropic modification of silicon was produced using a high-pressure precursor method<sup>10</sup>. This phase, called Si<sub>24</sub>, contains 24 silicon atoms distributed over three crystallographically unique Wyckoff positions in an orthorhombic *Cmcm* unit cell that is topologically

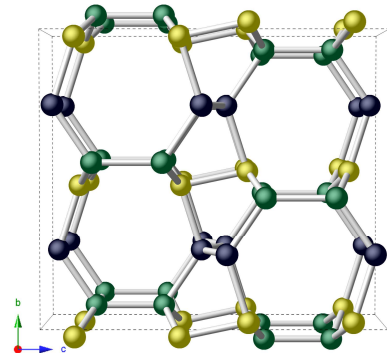


FIG. 1. (Color online) Unit cell of Si<sub>24</sub>, with colors indicating different crystallographic sites.

equivalent to the zeolite structure type CAS (see Fig. 1). In addition to the unique structure with large channels that propagate down the *a*-axis, the electronic structure is of particular interest. While Si<sub>24</sub> is formally an indirect band gap semiconductor (1.3 eV), the magnitude of a dipole-allowed direct gap is only a few hundredths of an eV greater than the indirect gap, suggesting potential for future photovoltaic and other optoelectronics applications.

The thermodynamic functions that determine the structure and properties of a material depend on atomic vibrations, quantized as phonons. Phonons are, in fact, responsible for the majority of entropy in most materials at moderate temperature and can give rise to anomalous changes in thermal and mechanical properties. The lattice dynamics of Si<sub>24</sub> are much less well understood than for DC-Si<sup>11-13</sup>. Total energy calculations based on density functional theory at zero temperature indicate that Si<sub>24</sub> is metastable with respect to DC-Si by only

<sup>\*</sup> xtong@caltech.edu

<sup>†</sup> xx2@caltech.edu

<sup>‡</sup> btf@caltech.edu

<sup>§</sup> hzhang@carnegiescience.edu

<sup>¶</sup> tstrobel@carnegiescience.edu

<sup>\*\*</sup> dkim@carnegiescience.edu

0.09 eV/atom at atmospheric pressure, and calculations of phonon dispersions indicate that Si<sub>24</sub> should remain mechanically stable up to 10 GPa<sup>10</sup>.

Unlike DC-Si which exhibits only one Raman-active, zone-center phonon ( $T_{2g}$ ), Si<sub>24</sub> possesses a rich Raman spectrum with 18 active modes ( $6A_g+3B_{1g}+3B_{2g}+6B_{3g}$ ) formally allowed by the crystal structure. A study of these modes under varying conditions of pressure and temperature provides the opportunity to approach thermodynamic quantities such as entropy, and provides insights into intrinsic mechanical and thermal properties. Related open-framework materials such as type-II clathrate (Si<sub>136</sub>) have been observed to exhibit interesting features such as negative mode Grüneisen parameters and negative thermal expansion at low temperatures<sup>14</sup>.

## I.2. Phonons at $T$ and $P$

It is generally expected that atomic vibrational frequencies increase with pressure. The Grüneisen parameter for the  $i$ th phonon mode is defined as fractional change of the phonon frequency per fractional change in volume

$$\gamma_i \equiv -\frac{V}{\omega_i} \left( \frac{\partial \omega_i}{\partial V} \right)_T. \quad (1)$$

Usually  $\gamma$  is expected to be a positive number, so frequencies are expected to increase (stiffen) with reductions in volume. When thermal phonon shifts are attributed solely to thermal expansion, the “quasiharmonic approximation” (QHA) is obtained<sup>15</sup>. The QHA assumes that phonon modes are harmonic, non-interacting, and their energies depend only on the volume of the crystal.

Another effect of temperature on vibrational frequencies in non-harmonic interatomic potentials is “anharmonicity,” which occurs even in the absence of thermal expansion. Effects of anharmonicity are found in molecular dynamics calculations at elevated temperatures, using accurate shapes of interatomic potentials.

An analytical approach to anharmonicity using many-body theory<sup>16–19</sup> is also successful for modest anharmonicity. The magnitude and sign of these shifts originate with “three-phonon” processes where one phonon transforms into two while conserving energy and momentum. Four-phonon processes can also be important. These “phonon-phonon interactions” are proportional to the strength of the cubic and quartic terms in the potential energy of the phonon mode. A key result from many-body theory that we exploit below is that the anharmonic shifts of phonon frequencies are linear with temperature, parameterized for the  $i$ th mode by

$$A_i \equiv \frac{1}{\omega_i} \left( \frac{\partial \omega_i}{\partial T} \right)_V. \quad (2)$$

A subtlety occurs in crystals with inversion symmetry at all atom sites, so an odd cubic term in the displacement potential is impossible. Nevertheless, the cubic term contributes in second order, where it competes

with the quartic term. For Si<sub>24</sub>, however, there are many vibrational modes having atom displacements without inversion symmetry, so the cubic term can occur in first order. This could give a large anharmonicity to Si<sub>24</sub>.

A separation of quasiharmonicity and anharmonicity is possible by assuming each vibrational frequency  $\omega_i(V, T)$  is a function of volume and temperature. For small changes in  $V$  or  $T$ , we expect a change in frequency

$$\Delta \omega_i = \left( \frac{\partial \omega_i}{\partial V} \right)_T \Delta V + \left( \frac{\partial \omega_i}{\partial T} \right)_V \Delta T. \quad (3)$$

The partial derivatives are identified with physical effects from the Grüneisen parameter  $\gamma_i$  of Eq. 1 and from the anharmonicity that causes frequency shifts with temperature

$$\Delta \omega_i = -\gamma_i \omega_i \frac{\Delta V}{V} + A_i \omega_i \Delta T. \quad (4)$$

The  $\Delta V$  in Eq. 4 originates with a change in applied pressure  $\Delta P$  and with a change in temperature  $\Delta T$  through thermal expansion

$$\frac{\Delta V}{V} = -\frac{\Delta P}{B} + \beta \Delta T, \quad (5)$$

where  $B$  is the bulk modulus and  $\beta$  the volume thermal expansivity. These two terms give the “quasiharmonic shifts” when substituted into Eq. 3. with quasiharmonicity and anharmonicity

$$\Delta \omega_i = -\gamma_i \omega_i \frac{\Delta P}{B} - \gamma_i \beta \Delta T \omega_i + A_i \omega_i \Delta T. \quad (6)$$

Equation 6 seems to work well when  $\Delta P$  and  $\Delta T$  are small. It has been much less explored when  $\Delta P$  and  $\Delta T$  are large, although the geophysics community has approached this problem in a number of ways<sup>20,21</sup>.

We performed Raman spectroscopy on Si<sub>24</sub> in a diamond-anvil cell at pressures from 0 to 8 GPa and simultaneously at temperatures between 80 K and 400 K. Frequency shifts were readily obtained for seven phonon modes, but the signs and magnitudes of these shifts were distinctly different. Furthermore, the data showed that the parameters  $\gamma_i$  and  $A_i$  in Eq. 6 could not be treated as constants. The Grüneisen parameters  $\gamma_i$  depend strongly on temperature, and the anharmonicity parameters  $A_i$  depend strongly on volume. Finally, implications for thermodynamic stability at high temperatures and pressures are suggested.

## II. METHODS

Samples of Si<sub>24</sub> were prepared as described previously<sup>10</sup>. In short, the polycrystalline Na<sub>4</sub>Si<sub>24</sub> precursor was prepared at 8 GPa and 1125 K and recovered to ambient conditions. Sodium was extracted under high vacuum at 400 K. After washing with ethanol and water, small ( $50 \times 50 \times 10 \mu\text{m}^3$ ) pieces of phase-pure Si<sub>24</sub> were selected from the bulk sample. The presence of

residual sodium within the structure was not detectable by powder X-ray diffraction, Raman spectroscopy measurements, or by X-ray spectroscopy methods employed previously<sup>10</sup>. We estimate the residual sodium content to be less than 0.1 at.% based on comparisons with previous measurements utilizing energy-dispersive X-ray spectroscopy<sup>10</sup>.

Raman spectroscopy measurements were performed in a gasketed, symmetric diamond-anvil cell (DAC) with helium used as the pressure-transmitting medium. Experiments were also performed using argon as the pressure medium (see supplemental information). A 532 nm diode laser was used as the excitation source and focused onto the sample using a 20× long-working-distance objective lens. The power at the sample was approximately 10 mW. Scattered light was collected in a 180° back-scatter geometry and focused onto a 50 mm confocal pinhole, which served as a spatial filter. This light was then passed through two narrow-band notch filters (Ondax, SureBlock), and focused onto the entrance slit of a spectrograph (Princeton Instruments, SP2750) in which light was dispersed by an 1800 gr/mm grating and detected with a liquid-nitrogen-cooled charge-coupled device (Princeton Instruments, Plyon). Pressure was measured using the ruby fluorescence method (quasi-hydrostatic scale)<sup>22</sup>. The DAC was placed in a liquid nitrogen cryostat for cooling and heating. Samples were measured at temperatures from 80 K to 400 K and pressures from 0 GPa to 8 GPa.

The Raman-active modes were calculated by density functional perturbation theory as described previously<sup>10</sup>. A Brillouin zone sampling grid with  $2\pi \times 0.04 \text{ \AA}^{-1}$  intervals was used with a plane basis set cutoff of 500 eV. The Raman frequencies were calculated for zero temperature in the harmonic approximation, and the results were compared successfully to experimental frequencies in Ref. 10. To obtain mode Grüneisen parameters  $\gamma_{i,\text{DFT}}$  as defined in Eq. 1, Raman frequencies were calculated at rescaled volumes of the unit cell, corresponding to a pressure range of approximately 1 GPa.

### III. RESULTS

Six representative Raman spectra of Si<sub>24</sub> are shown in Fig. 2. The Raman spectrum at 80 K under 0 GPa pressure appears to have 11 peaks, but the ninth peak (with the  $A_g^{(5)}$ ) consists of two overlapping peaks. All twelve Raman-active modes from  $B_{1g}$ ,  $B_{2g}$ ,  $B_{3g}$  and  $A_g$  in the spectra were used to qualitatively analyze the effect of temperature and pressure on line positions. At elevated temperatures and pressures, several of the weak modes either could not be resolved from the background, or their positions could not be determined reliably. Seven peaks from 1  $B_{3g}$ , 1  $B_{1g}$  and 5  $A_g$  modes were sufficiently distinct to allow quantitative measurements of their frequencies, which were in a good agreement with prior experimental and theoretical results<sup>10</sup>. After background

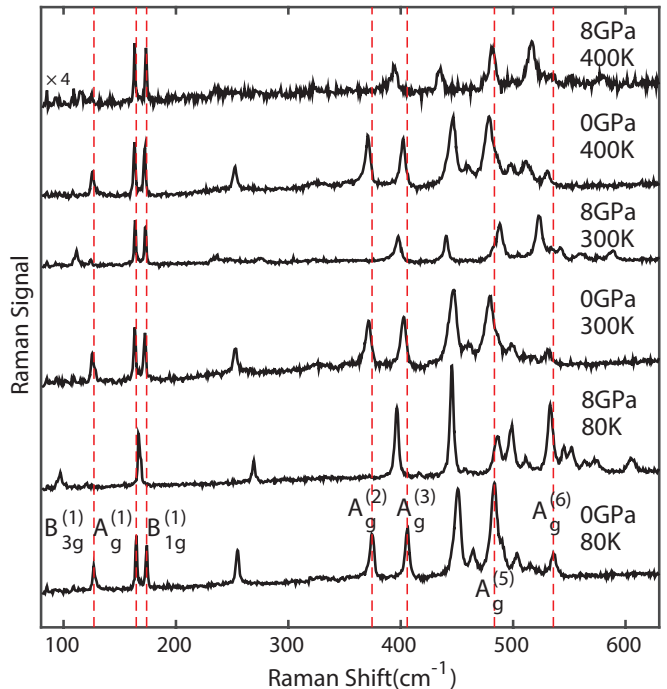


FIG. 2. (Color online) Raman spectra of Si<sub>24</sub> at selected temperatures and pressures.

subtraction, the spectral peaks were fitted to Lorentzian functions to find their centroids, which are presented in Table I.

The fractional shifts of frequency with pressure and temperature are shown in Fig. 3. For all modes with frequencies  $\omega > 200 \text{ cm}^{-1}$ , the Raman frequencies stiffen with increased pressure and soften with increased temperatures, as is normally expected. The mode  $B_{3g}^{(1)}$  of lowest energy shows the opposite trend, however, and the mode  $B_{1g}^{(1)}$  shows this anomalous tendency, to a lesser degree. In Fig. 3a the effects of temperature are shown with arrows. Temperature causes a reduction of the pressure shifts for all modes, but these changes are in opposite directions for the low- and high-energy modes.

Figure 3b shows the temperature-dependence of the Raman modes. At a pressure of 0 GPa, all modes decrease with temperature in a conventional way, as indicated by the solid (red) curve. At a pressure of 8 GPa, however, the temperature dependence of all modes become different, with the  $B_{3g}^{(1)}$  and  $B_{1g}^{(1)}$  modes showing a peculiar thermal stiffening.

For working with experimental data, the mode Grüneisen parameter of Eq. 1 can be written as

$$\gamma_{iT} = \frac{B}{\omega_i} \left( \frac{\partial \omega_i}{\partial P} \right)_T. \quad (7)$$

These mode Grüneisen parameters are functions of volume alone, and are comparable to the calculated parameters  $\gamma_{i,\text{DFT}}$  listed in Table II. As shown in Fig. 3a, the curvatures of  $B_g$  modes indicate a noteworthy pressure

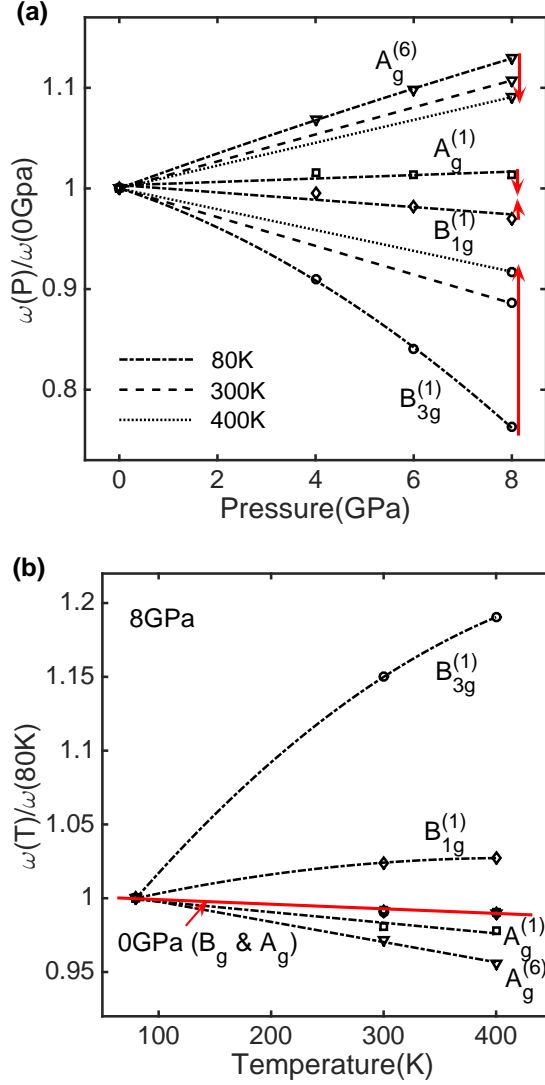


FIG. 3. (a) Fractional frequency shifts of Raman modes with pressure. The  $A_g$  modes stiffen under higher pressure as generally expected, but the  $B_g$  modes soften. The arrows at the ends of the curves show the change of  $\omega(P)/\omega(0 \text{ GPa})$  between 80 K and 400 K. (b) Fractional frequency shifts of Raman modes with temperature. The red curve is common for all four modes at a pressure of 0 GPa. The black curves are for 8 GPa. Note the anomalous thermal stiffening of the  $B_{3g}^{(1)}$  and  $B_{1g}^{(1)}$  modes at 8 GPa.

dependence of Grüneisen parameters. These are shown in Fig. 4 for several modes. The results summarized in Fig. 5 and Table II show the different pressure-dependent anharmonicities of Raman active modes.

#### IV. DISCUSSION

The mode Grüneisen parameter  $\gamma_i$  (Eq. 7) accounts for frequency shifts with volume at constant temperature. A complementary phenomenon from phonon-phonon anharmonicity is the frequency shift with tem-

TABLE I. Frequencies of Raman modes labeled in Fig. 2.

Mode	80 K		300 K		400 K	
	0 GPa	8 GPa	0 GPa	8 GPa	0 GPa	8 GPa
$B_{3g}^{(1)}$	127.1	96.9	125.8	111.4	125.8	115.4
$A_g^{(1)}$	164.7	166.9	163.4	163.7	163.1	163.2
$B_{1g}^{(1)}$	173.9	168.8	172.3	172.8	172.2	173.3
$A_g^{(2)}$	374.5	396.5	371.2	397.5	370.7	394.0
$A_g^{(3)}$	405.8	445.5	402.4	440.4	401.9	434.8
$A_g^{(5)}$	483.4	533.1	479.3	523.1	478.4	516.3
$A_g^{(6)}$	535.8	605.4	531.1	588.1	530.4	578.6

perature at constant volume<sup>16,18,19,23</sup>. At low pressures, these mode anharmonicities  $A_i$  can be isolated from the effects of thermal expansion when the Grüneisen parameter is known<sup>21</sup>. Such an analysis with independent terms linear in  $\Delta T$  and  $\Delta P$  proved too restrictive for the present data set because the parameters changed as shown in Figs. 4 and 5. We were forced to use a more general analysis of the phonon frequencies.

We allowed higher-order  $P-T$  dependences for the Raman modes. Starting with Eq. 6, the frequency variation with  $P$  and  $T$  can be written as

$$\frac{\Delta\omega_i}{\omega_i} = -\gamma_i \frac{\Delta P}{B} - \gamma_i \beta \Delta T + A_i \Delta T. \quad (8)$$

Using definitions of  $\gamma_i$  and  $A_i$  in Eq. 1 and Eq. 2, and the additional definitions

$$g_T \equiv V \left( \frac{\partial \gamma}{\partial V} \right)_T = -B \left( \frac{\partial \gamma}{\partial P} \right)_T$$

$$a_T \equiv V \left( \frac{\partial A}{\partial V} \right)_T = -B \left( \frac{\partial A}{\partial P} \right)_T$$

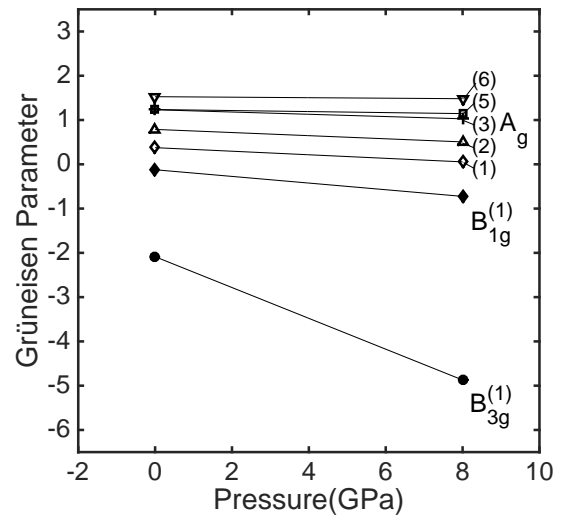


FIG. 4. Fitted mode Grüneisen parameters  $\gamma_i$  for selected seven modes as a function of pressure at 0 K, where  $B_g$  and  $A_g$  modes are denoted with the solid markers and open markers respectively.

the mode frequency  $\omega_i$  is a second order function of pressure and temperature, as shown in the Supplemental material<sup>24</sup>

$$\frac{\Delta\omega_i}{\omega_i} = \left[ \frac{\gamma_{i0}}{B} \Delta P \right]_1 + [(A_{i0} - \gamma_{i0}\beta)\Delta T]_2 - \left[ \frac{a_{iT}}{B} \Delta T \Delta P \right]_3 - \left[ \frac{g_{iT}}{2B^2} (\Delta P)^2 \right]_4 \quad (9)$$

The first two terms in square braces, linear in  $\Delta P$  and  $\Delta T$ , are essentially the same as Eq. 4. The bulk modulus  $B$  was set to 90 GPa for the open framework clathrate silicon<sup>25</sup> and we used the volume thermal expansion coefficient  $\beta = 1.2 \times 10^{-5} \text{ K}^{-1}$  reported by Kurakevych, *et al.*<sup>26</sup>.

The two parameters of Eq. 9 for selected modes were assessed by fitting to all experimental data from a Raman mode, and results are given in Table II. Using these parameters, the four terms in square braces in Eq. 9, labeled as [1], [2], [3], [4], (with numbers corresponding to subscripts on the square brackets in Eq. 9) were calculated, and Fig. 6 gives their contributions for  $\Delta\omega/\omega$  for the range of  $\Delta P = 8 \text{ GPa}$  and  $\Delta T = 320 \text{ K}$ .

As expected, the pure pressure dependence of term [1] gives the dominant contribution to  $\Delta\omega/\omega$ . What is surprising is that the term [3], proportional to  $\Delta P \Delta T$  is also a main contributor to  $\Delta\omega_i/\omega_i$  for the  $B_g$  modes.

Energetic considerations are perhaps appropriate. In a temperature interval of  $\Delta T = 320 \text{ K}$ , the change in characteristic thermal energy is  $k_B \Delta T = 27 \text{ meV/atom}$ , and a change in pressure of 8 GPa corresponds to an energy  $P \Delta V = 100 \text{ meV/atom}$ . For both modes  $B_g$  and  $A_g$ , the shifts from  $\Delta P$  are larger than that from  $\Delta T$ . Nevertheless, thermal phonon-phonon anharmonicity is surprisingly large in  $\text{Si}_{24}$  at these low temperatures, perhaps owing to the low symmetry of the clathrate crystal

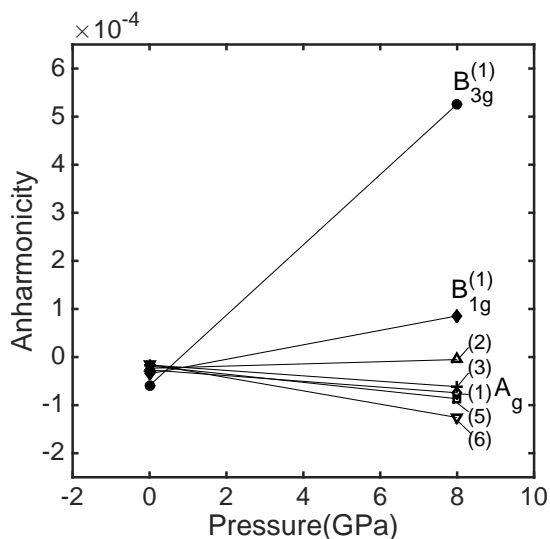


FIG. 5. Fitted anharmonicity parameters  $A_i$  for selected seven modes as a function of pressure at 0 K, where  $B_g$  and  $A_g$  modes are denoted with the solid markers and open markers respectively.

TABLE II. Grüneisen parameters, anharmonicity parameters and their first order derivatives defined in Eq. 9. All values are evaluated at the initial condition ( $T_0 = 0 \text{ K}$ ,  $P_0 = 0 \text{ GPa}$ ).

	$\gamma_i$	$A_i$ $\text{K}^{-1}$	$-g_{iT}/B$ $\text{GPa}^{-1}$	$-a_{iT}/B$ $(\text{K GPa})^{-1}$	$\gamma_{i,\text{DFT}}$ at 1 GPa
$B_{3g}^{(1)}$	-2.087	$-5.913 \times 10^{-5}$	-0.348	$7.313 \times 10^{-5}$	-1.80
$A_g^{(1)}$	0.376	$-2.677 \times 10^{-5}$	-0.040	$-0.594 \times 10^{-5}$	0.10
$B_{1g}^{(1)}$	-0.123	$-3.477 \times 10^{-5}$	-0.075	$1.505 \times 10^{-5}$	-0.71
$A_g^{(2)}$	0.788	$-2.333 \times 10^{-5}$	-0.035	$0.227 \times 10^{-5}$	0.66
$A_g^{(3)}$	1.232	$-1.658 \times 10^{-5}$	-0.026	$-0.563 \times 10^{-5}$	1.08
$A_g^{(5)}$	1.237	$-1.866 \times 10^{-5}$	-0.012	$-0.850 \times 10^{-5}$	1.15
$A_g^{(6)}$	1.527	$-1.483 \times 10^{-5}$	-0.006	$-1.387 \times 10^{-5}$	1.42

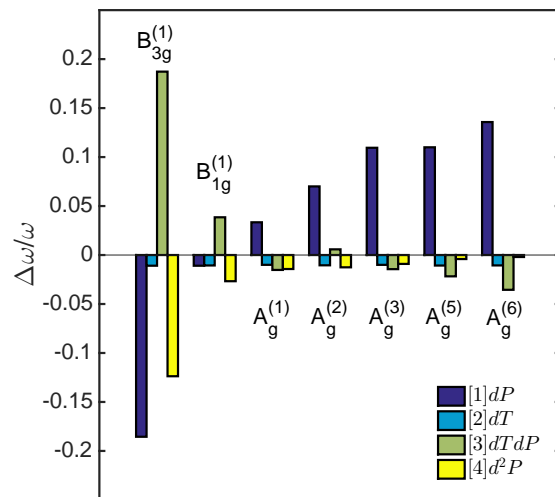


FIG. 6. Contributions to frequency shifts from five terms in Eq. 9 with  $\Delta P = 8 \text{ GPa}$ ,  $\Delta T = 320 \text{ K}$ .

structure. More surprising, however, is the large effect of term [3], proportional to  $\Delta P \Delta T$ , on the phonon frequency shift of the  $B_{3g}^{(1)}$  mode.

Phonon shifts proportional to  $\Delta P \Delta T$  could, conceptually, arise from a temperature dependence of the Grüneisen parameter, or a pressure dependence of the anharmonicity from phonon-phonon interactions. Both are proportional to  $(V/\omega_0) \partial^2 \omega / (\partial T \partial V)$ , so we interpret both cross-terms with  $a_{iT}$  as follows. Phonon-phonon anharmonicity originates from processes where a phonon is created or annihilated as it absorbs, or emits, two or more other phonons. These elementary processes must satisfy kinematical conditions that conserve energy and momentum, and these kinematical conditions depend on details of the phonon dispersions in the material. Because the phonons in different dispersions have different Grüneisen parameters, the separations in energy and momentum of the phonons will change with  $\Delta P$ , contributing to  $a_{iT}$ . The vertex interactions that give the strengths of phonon-phonon interactions may also change with  $\Delta P$ .

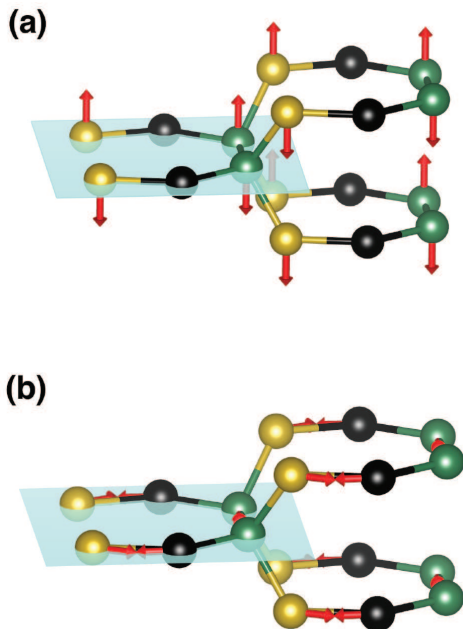


FIG. 7. Vibrational motions of (a)  $B_{3g}^{(1)}$  and (b)  $A_g^{(6)}$ .

The atom displacements in the  $B_{3g}^{(1)}$  and  $A_g^{(6)}$  modes, obtained from the DFT calculations, are shown in Fig. 7. The interlayer  $B_{3g}^{(1)}$  vibrational mode involves more bending of interatomic bonds, whereas bond stretching dominates most other modes such as  $A_g^{(6)}$ . It is typical for bond stretching in solid crystals to be associated with positive Grüneisen parameters and positive thermal expansion<sup>27</sup>. When the displacements between a neighboring pair of atoms lie along the direction of their separation as in Fig. 7b, the atoms spend more time in the softer part of their interatomic potential, which is at larger separations. Thermal expansion is expected, and the frequencies soften with temperature as does the  $A_g^{(6)}$  mode, for example.

Compared to the  $A_g$  modes, the  $B_{3g}^{(1)}$  and  $B_{1g}^{(1)}$  modes involve more bending of bonds than stretching of bonds. Sometimes these bending modes are associated with anomalous Grüneisen parameters and even with negative thermal expansion<sup>28–30</sup>, but proper interpretations would require full molecular dynamics simulations. Nevertheless, it seems possible that the bond bending dynamics of the  $B_{3g}^{(1)}$  mode could be responsible for its negative Grüneisen parameter<sup>31</sup>. It is surprising, however, that the  $B_{3g}^{(1)}$  mode softens so strongly with compression, and this occurs at low temperatures where the phonon occupancy is small (See Supplemental material<sup>24</sup> Fig. 1). At higher temperatures, and larger atom displacements in the  $B_{3g}^{(1)}$  mode, this anomalous behavior is reduced in magnitude.

Atom vibrations are the largest contributor to the ther-

modynamic entropy of  $\text{Si}_{24}$ , as they are for diamond cubic Si. A comparison is interesting. Diamond cubic Si has a large pure anharmonicity at ambient pressure, several times larger than quasiharmonic effects from thermal expansion<sup>13</sup>. At ambient pressure, the average thermal shift of the phonon modes of  $\text{Si}_{24}$  (red line in Fig. 3b) is nearly the same as for the phonons in diamond cubic Si, measured by inelastic neutron scattering. At ambient temperature, the pressure shift of the  $A_g^{(6)}$  mode of  $\text{Si}_{24}$  is approximately the same as the pressure shift of the single Raman mode of diamond cubic Si<sup>12</sup>, although these authors also report some negative Grüneisen parameters for two-phonon Raman features.

The clathrate structure of  $\text{Si}_{24}$  transforms to the  $\beta$ -Sn structure above 12 GPa and 300 K, which is not far outside our range of measurements. The transformation depends on properties of the  $\beta$ -Sn structure, but it is plausible that it is more stable than the clathrate structure at all temperatures and pressures. The transformation could be facilitated by the larger amplitudes of low-energy phonon modes in the clathrate structure that occur with increased pressure.

The vibrational entropy depends on all phonon modes in a material, and we have measured only seven of them. Nevertheless, the present results indicate that under simultaneous  $T$  and  $P$ , the thermodynamic entropy of  $\text{Si}_{24}$ , and likely other materials, cannot be reliably obtained by adding contributions from effects of  $T$  and  $P$  alone.

## V. CONCLUSION

The different Raman-active phonon modes in  $\text{Si}_{24}$  have markedly different shifts in frequency with volume and with temperature. The low-energy bending modes have frequency shifts of opposite sign with  $P$  and  $T$  as the higher-energy stretching modes. Over a range of  $T$  of 320 K and a range of  $P$  of 8 GPa, the effects of temperature and pressure caused comparable shifts of Raman modes. However, for the  $B_{3g}^{(1)}$  and  $B_{1g}^{(1)}$  modes the Grüneisen parameters  $\gamma_i$  depended strongly on temperature, and the anharmonicity parameters  $A_i$  depended strongly on volume. Consequently, the frequency shifts proportional to  $\Delta P \Delta T$  were comparable to the effects of  $\Delta P$  and  $\Delta T$  alone. The thermodynamic entropy of  $\text{Si}_{24}$  likely depends significantly on the product  $\Delta T \Delta P$ , and not just on  $\Delta T$  and  $\Delta P$  alone.

## VI. ACKNOWLEDGMENT

This work was supported as part of the Energy Frontier Research in Extreme Environments (EFREE) Center, an Energy Frontier Research Center funded by the US Department of Energy, Office of Science under Award Number DE-SC0001057.

- 
- <sup>1</sup> B. Zheng, J. Michel, F. Ren, L. Kimerling, D. Jacobson, and J. Poate, *Applied Physics Letters* **64**, 2842 (1994).
- <sup>2</sup> W. L. Ng, M. Lourenco, R. Gwilliam, S. Ledain, G. Shao, and K. Homewood, *Nature* **410**, 192 (2001).
- <sup>3</sup> S. G. Cloutier, P. A. Kossyrev, and J. Xu, *Nature Materials* **4**, 887 (2005).
- <sup>4</sup> M. Fujita, *Nature Photonics* **7**, 264 (2013).
- <sup>5</sup> S. Botti, J. A. Flores-Livas, M. Amsler, S. Goedecker, and M. A. Marques, *Physical Review B* **86**, 121204 (2012).
- <sup>6</sup> A. Mujica, C. J. Pickard, and R. J. Needs, *Physical Review B* **91**, 214104 (2015).
- <sup>7</sup> M. Amsler, S. Botti, M. A. Marques, T. J. Lenosky, and S. Goedecker, *Physical Review B* **92**, 014101 (2015).
- <sup>8</sup> Q. Zhu, A. R. Oganov, A. O. Lyakhov, and X. Yu, *Physical Review B* **92**, 024106 (2015).
- <sup>9</sup> B. Haberl, T. Strobel, and J. Bradby, *Appl. Phys. Rev.* **3**, 040808 (2016).
- <sup>10</sup> D. Y. Kim, S. Stefanoski, O. O. Kurakevych, and T. A. Strobel, *Nature Materials* **14**, 169 (2015).
- <sup>11</sup> T. Hart, R. Aggarwal, and B. Lax, *Physical Review B* **1**, 638 (1970).
- <sup>12</sup> B. A. Weinstein and G. J. Piermarini, *Physical Review B* **12**, 1172 (1975).
- <sup>13</sup> D. Kim, H. Smith, J. L. Niedziela, C. Li, D. L. Abernathy, and B. Fultz, *Physical Review B* **91**, 014307 (2015).
- <sup>14</sup> X. Tang, J. Dong, P. Hutchins, O. Shebanova, J. Gryko, P. Barnes, J. K. Cockcroft, M. Vickers, and P. F. McMillan, *Physical Review B* **74**, 014109 (2006).
- <sup>15</sup> M. T. Dove, *Introduction to Lattice Dynamics*, Vol. 4 (Cambridge University Press, 1993).
- <sup>16</sup> A. A. Maradudin and A. E. Fein, *Physical Review* **128**, 2589 (1962).
- <sup>17</sup> R. Cowley, *Advances in Physics* **12**, 421 (1963).
- <sup>18</sup> D. C. Wallace, *Thermodynamics of Crystals* (Dover Publications, 1998).
- <sup>19</sup> D. C. Wallace, *Statistical Physics of Crystals and Liquids: a guide to highly accurate equations of state* (World Scientific, 2003).
- <sup>20</sup> O. L. Anderson, *Equations of State of Solids for Geophysics and Ceramic Science* (Oxford University Press, 1995).
- <sup>21</sup> R. Hemley, *Ultrahigh-Pressure Mineralogy: Physics and Chemistry of the Earth's Deep Interior*, Reviews in Mineralogy, Vol. 37 (Mineralogical Society of America, 1998) pp. 525–559.
- <sup>22</sup> H. Mao, J.-A. Xu, and P. Bell, *Journal of Geophysical Research: Solid Earth* **91**, 4673 (1986).
- <sup>23</sup> B. Fultz, *Progress in Materials Science* **55**, 247 (2010).
- <sup>24</sup> See Supplemental material for the derivation of generalized model of Eq. 9 and more experimental data (2016).
- <sup>25</sup> A. San-Miguel, P. Kéghélian, X. Blase, P. Mélinon, A. Perez, J. Itié, A. Polian, E. Reny, C. Cros, and M. Pouchard, *Physical Review Letters* **83**, 5290 (1999).
- <sup>26</sup> O. O. Kurakevych, T. A. Strobel, D. Y. Kim, T. Muramatsu, and V. V. Struzhkin, *Crystal Growth & Design* **13**, 303 (2012).
- <sup>27</sup> F. Cerdeira, C. J. Buchenauer, F. H. Pollak, and M. Cardona, *Physical Review B* **5**, 580 (1972).
- <sup>28</sup> W. Miller, C. W. Smith, D. S. Mackenzie, and K. E. Evans, *Journal of Materials Science* **44**, 5441 (2009).
- <sup>29</sup> T. Mary, J. Evans, T. Vogt, and A. Sleight, *Science* **272**, 90 (1996).
- <sup>30</sup> C. H. Xu, C. Z. Wang, C. T. Chan, and K. M. Ho, *Physical Review B* **43**, 5024 (1991).
- <sup>31</sup> C. W. Li, X. Tang, J. A. Munoz, J. B. Keith, S. J. Tracy, D. L. Abernathy, and B. Fultz, *Physical Review Letters* **107**, 195504 (2011).